Reply on RC2

Q: Line 26: The increases in AR frequency over the Arctic are not spatially uniform, with faster increases over the Atlantic sector (Ma et al., 2024a).
A: We thank the reviewer for this comment. We have incorporated the remark as follow: '*However, these trends exhibit substantial regional variability (Wang et al., 2024; Zhang et al., 2023), with AR frequency over the North Atlantic increasing at roughly twice the rate as over the Pacific in recent decades (Ma et al., 2024a).*' See line 40-42 on page 2.

Q: Line 211: 'Coinciding' is not very accurate here. It seems that Q2m begins to decline sharply only after precipitation returns to ~0. Please explain why the decline in Q2m lags behind changes in precipitation.
A: To address this comment, we have rewritten the relevant part as follows: '*A spike in total precipitation occurs while the Eurasian AR remains above the ship on 16 April (Fig. 3e), followed by a sharp decline in Q2m due to the removal of atmospheric moisture through precipitation, and accompanied by a marked decrease in SEB.*' See line 241-243 on page 11.

Q: Fig. 2a: The results shown here are consistent with the findings of Ma et al. (2024b) (see their Fig. 10). Arctic ARs are usually driven by a cyclone–anticyclone couplet. This couplet can be further divided into a high-pressure-dominant regime (associated with the Siberian AR), with a relatively weak low-pressure system to the left, and a low-pressure-dominant regime (associated with the Atlantic AR), with a relatively weak high-pressure system to the right. I think the authors should provide additional discussion in the Introduction on the flow regimes that drive Arctic AR formation. This would give readers more context for interpreting the results presented in this study.
A: We thank the reviewer for this comment and for drawing our attention to the study by Ma et al. (2024b). In response, we have expanded the Introduction section to include a description of the flow regimes associated with Arctic ARs, as well as a brief classification of the cyclone-anticyclone couplets driving the Atlantic and Eurasian ARs. The revised text reads:
'*Further, three distinct circulation patterns driving Arctic ARs have been identified: a dipole pattern, featuring high (low) pressure anomalies on the east (west) side of the AR; an anticyclone-dominated regime, characterised by a strong, persistent anticyclone on the east side of AR with a weak cyclone on the west; and a cyclone-dominated regime, characterised by a pronounced cyclone on the east side of the AR and weaker anticyclone on the west side (Ma et al., 2024b).*' See lines 32-36 on page 2.

'*This circulation pattern is consistent with the cyclone-dominant regime identified by Ma et al. (2024b).*' See lines 221-222 on page 9.

'*This cyclone–anticyclone couplet corresponds to the anticyclone-dominated regime, which was the most common, accounting for approximately 40% of the events analysed by Ma et al. (2024b) and linked to the strongest and most spatially extensive surface warming anomalies.*' See line 226-229 on pages 9-10.

Q: Fig. 5b: Sea-ice concentration decreases of comparable magnitude can also be observed in the marginal sea-ice regions of the Pacific sector. However, ARs were not observed in those regions. Is it possible that the sea-ice reduction shown in Fig. 5b is simply driven by the seasonality of sea-ice melt? Please also examine the sea-ice concentration differences between 12 April and 22 April in years when no AR event influenced these regions.

A: During the analysed period, a third Arctic AR occurred over western Canada where negative SIC changes in the Pacific sector can be seen in Fig. 5b. This AR was not included in our analysis, as it did not pass over the MOSAiC site, and we therefore lack the in-situ measurements required to study it consistently alongside the other two AR events. The SIC reductions in the Pacific sector during this period may be linked to this additional AR, though we acknowledge that SIC variability is influenced by many factors, including ocean temperature anomalies, wind speeds, and preceding sea-ice conditions, and it is beyond the scope of this study to fully explain all elements of this variability. We have clarified this point in the revised manuscript and added a sentence acknowledging that the impact of ARs on sea-ice conditions needs more detailed investigation in future studies: '*Additionally, the impact of ARs on sea ice variability requires more detailed investigation, given the many interacting factors that govern sea ice change.*' See lines 481-482 on page 24.

To place the SIC changes in context, addressing the latter part of the above comment, we compared SIC for April 2020 to the 2005–2025 climatology over the SEG and BKS regions (see both figures below). In SEG, SIC in April 2020 is anomalously low, falling below one standard deviation of the mean. SIC declines slowly at the start of the month, but an accelerated decrease is apparent following the AR event. In BKS, by contrast, SIC is initially above the climatological mean in early April 2020 before undergoing a rapid decline during the AR event, falling from 0.56% on 14 April to 0.43% on 25 April, thus, markedly faster than the gradual climatological decline.

We have added a sentence to the manuscript, discussing these points: '*SIC gradually decreases and remains anomalously low throughout the month, falling below the ± 1 s.d. range of the April 2005–2025 climatology (not shown). (…) While SIC is above the climatological mean in early April, a rapid and exceptional decline is observed during the AR period compared to the typical cycle (not shown).*' See lines 295-305 on pages 13-14.

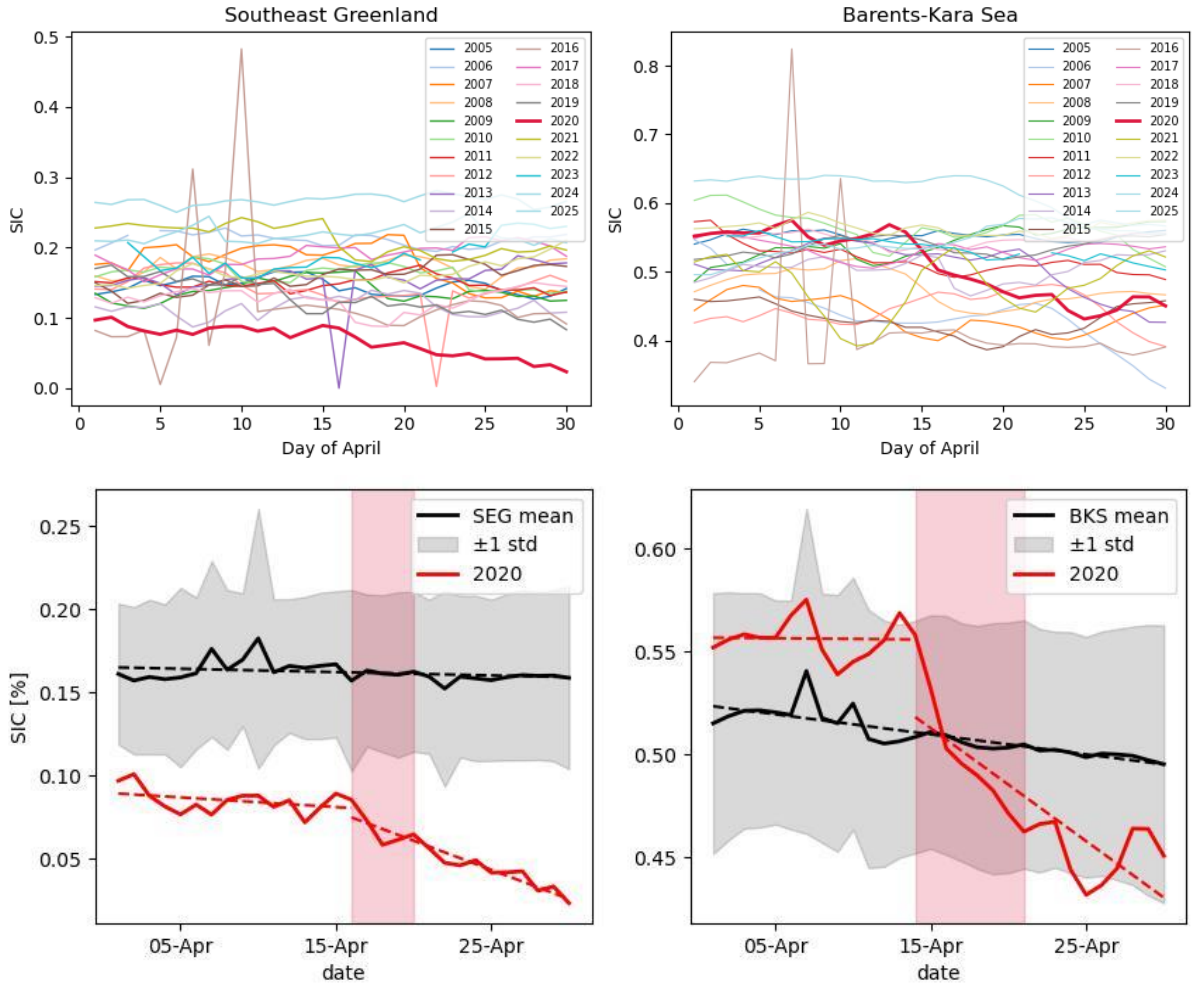

Q: Fig. 6c: What drives the precipitation peaks prior to the occurrence of ARs? Are they also driven by extreme moisture-transport events that are not captured by the Guan and Waliser (2024) AR detection algorithm? I recommend that the authors also plot IVT evolution in Fig. 1 using shaded contours and use line contours to indicate SLP anomalies. This would allow readers to assess whether these precipitation peaks are also associated with enhanced moisture transport.

A: Thank you for this comment. The precipitation peaks prior to the main AR events are indeed associated with ARs in the Guan and Waliser AR catalogue. Specifically, the catalogue identifies ARs over SEG on 05-06 April, 12-13 April and 21-22 April, which correspond directly to the spikes in precipitation visible in Fig. 6c. We have added a brief explanation of this in the revised figure caption and main text: '*The time series further reveal that notable precipitation and rainfall events occur outside the period when the ARs are located over SEG, coinciding with other Arctic ARs passing over the region on 05–06, 12–13, and 21–22 April (not shown).*' See lines 298-300 on page 13-14. We have made a figure with IVT as shaded contours and MSLP anomalies as line contours (see figure below) following the reviewer's suggestion. This additional plot clearly shows that the precipitation peaks on 13 and 21 April over the SEG region do

indeed coincide with high IVT. While the Guan and Waliser catalogue identifies them as ARs, we have only selected those AR contours that correspond to the Arctic ARs that are the focus of the present study. Including all detected ARs at each timestep would substantially overcrowd the figure, particularly given that the Guan and Waliser algorithm is relatively permissive compared to other AR detection tools, with multiple ARs commonly identified simultaneously over high latitudes (Shields et al., 2018; Rutz et al., 2019).

The figure shown below depicts enhanced IVT over multiple regions in the high latitudes such as over Alaska and the Atlantic. Including this figure in the main manuscript would shift focus away from the ARs analysed here. Further, as the first section of the results centres on the synoptic-scale cyclone and anticyclone evolution that steers the two ARs into the Arctic and their extreme nature, we retain MSLP as filled contours in Fig. 1.

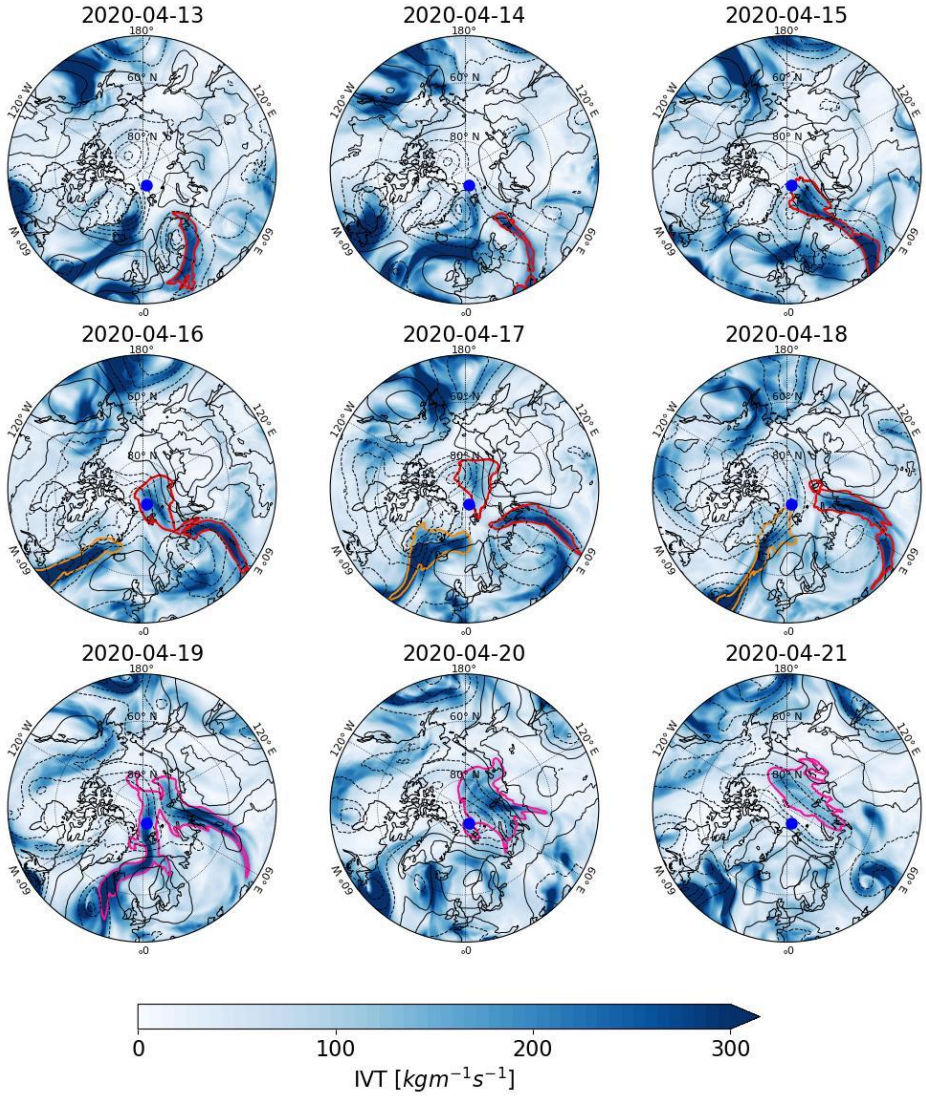

Q: Lines 267-268: Based on Fig. 6d, precipitation starts to increase and peaks after the passage of the AR.

A: We thank the referee for pointing this out. The sentence has been altered as follows: '*Following the AR retreat, precipitation increases substantially.*' See lines 308-309 on page 14.

Q: Fig. 9 caption: Should be "moisture uptake minus the absolute magnitude of moisture loss"?
A: The caption has been modified for the respective subplots of figures 9 and 12 according to the suggestion and now read: '*Moisture uptake minus absolute loss*'.

Q: Line 346: I can see the strong moisture loss in the figure. However, I don't see how strong upward motion is reflected in the figures. Additional explanations might be helpful here.
A: We thank the referee for this comment. The sentence has been modified as follows: '*Moisture loss accompanied by upward motion also occurs along the Atlantic pathway towards Iceland (Fig. 12b,d). Additionally, strong moisture loss and upward motion is shown over the Greenland coast.*' See lines 387-389 on page 19.

Q: Fig. 5: I suggest that the authors also plot the spatial distribution of precipitation intensity. This would help readers better understand the magnitude of extreme precipitation associated with Arctic ARs.
A: When preparing Fig. 5, we carefully considered how to best visualise extreme precipitation associated with the Arctic ARs, noting that precipitation in the high latitudes can be classified as an extreme event despite its small absolute magnitude. This issue became evident when examining precipitation during the target period over the central Arctic. Plotting the absolute precipitation amounts or cumulative totals for the target period 15-21 April 2020 (has now been added as panel a to Fig. 5, also see below), shows that the total precipitation over the central Arctic is of very small magnitude (<0.03 mm) in comparison to that over lower latitudes. Similarly, precipitation anomalies in polar regions are typically modest because the climatological precipitation rates there are very low and deviations from the climatological mean still translate to small absolute differences. For this reason, maps of precipitation intensity can be difficult to interpret in the Arctic context.
This was the reasoning behind our decision to plot the gridded precipitation percentile for the target period relative to all 7-day accumulated precipitation values for April 1979–2023. We further used a specific colour bar with a custom centre point to draw the reader's attention to high percentiles, i.e. extreme precipitation occurrences. This approach allowed us to highlight how unusual the observed precipitation over the central Arctic was with percentiles exceeding the 90th percentile.
Nonetheless, in response to the reviewer's recommendation, we have included the cumulative precipitation field as an additional panel to Fig. 5 to provide readers with a

clearer visual representation of the spatial distribution of precipitation associated with the analysed AR events.

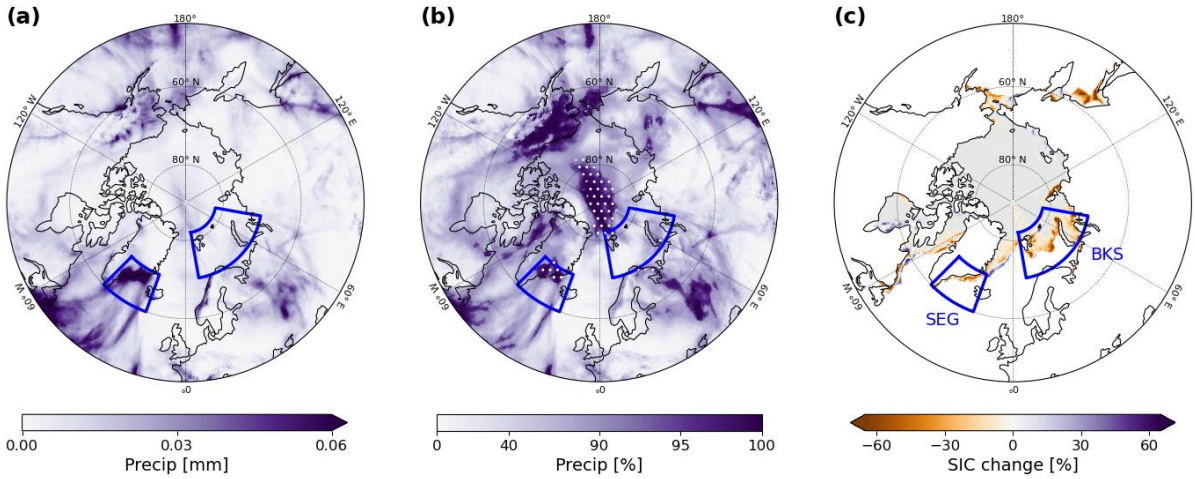

The revised manuscript now reads: '*Figure 5a shows that precipitation is particularly enhanced along the southeastern coast of Greenland, when accumulated over the target period, highlighting the key role of orographic uplift from the steep topography of Greenland in driving extreme precipitation events. In contrast, precipitation over the central Arctic remains relatively low compared to lower latitudes. When expressed as percentiles relative to the climatological distribution at each grid point (Fig. 5b), however, precipitation across the central Arctic is highly unusual, exceeding the 90th percentile and coinciding with areas where ARs persisted for at least three days (Fig. 4a). Precipitation along the southeastern Greenland coast is also highly anomalous relative to its climatology.*' See lines 274-279 on page 12.

Q: Fig. 7: Please explain how you calculated this spatial density distribution for parcel trajectories. This can help readers better interpret the results.
A: We have expanded on the explanation of the spatial density distribution plots. The figure caption for Fig. 7 now reads: '(...) *(b) Spatial density distribution of nTpΘ trajectories, obtained by binning all trajectory longitude–latitude positions into 2 °× 2 ° grid cells and computing a normalised two-dimensional histogram. Values represent the probability density of trajectory positions*.'

Q: Fig. 10: Since all these parcels are released in central Arctic, shouldn't central Arctic have the highest density distribution?
A: We thank the reviewer for pointing this out. Indeed, the central Arctic has the highest trajectory density, as this is where all parcels converge over a relatively small area. For Fig. 10, we computed densities on a 2°×2° latitude-longitude grid. When visualized on a Plate Carree projection, the bins appear equal in size, but their physical area is smaller at higher latitudes, effectively reducing the density at high latitudes (less parcels are counted in bins of smaller size). Plotting the density field on a North Polar

Stereographic projection clearly shows the effect of shrinking bin sizes with latitude (see figure below, left panel). This is the reason why the central Arctic does not appear as the region of highest density in Fig. 10.
To look further into this, we redefine the grid to consist of equal-sized bins in the North Polar Stereographic projection. In this representation, the central Arctic clearly shows the highest density compared to lower latitudes, reflecting the actual concentration of parcels. Note that now the bins appear to represent the same area in the NorthPolarStereo projection, but bins at lower latitudes are now smaller in physical size. Also, keep in mind that both figures below include all trajectories reaching the central Arctic with precipitation ±90th percentile, without any additional grouping based on ΔT or Δθ.
As the difference in density is somewhat striking, we will redo Figures 7 and 10 by taking the actual bin size into account. For now, we have added a sentence to the figure caption of Fig. 7 to clarify this binning/projection issue: *'Note that grid cell area decreases with latitude, such that bins at higher latitudes are smaller than those at lower latitudes. As a result, lower-latitude bins tend to contain more parcels and exhibit higher apparent densities, while higher-latitude bins contain fewer parcels and appear less dense.'*

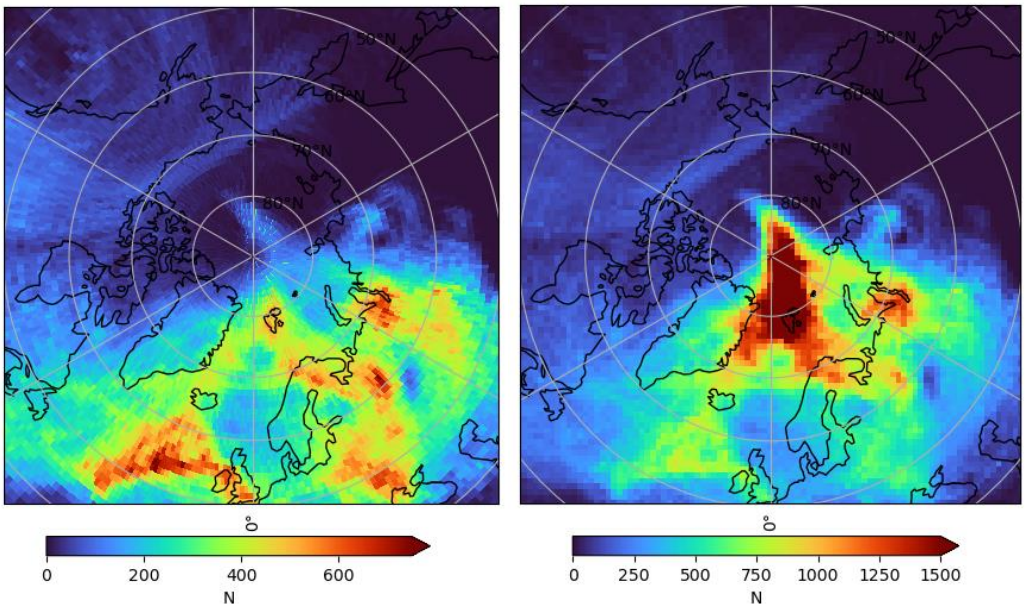

Q: Fig. 12: Please explain why there is a lack of moisture loss over the central Arctic where extreme AR precipitation occurs, and parcels are released.
A: We thank the reviewer for this comment. The apparent lack of moisture loss over the central Arctic reflects the very small absolute precipitation amounts in this region, consistent with the reviewer's earlier observation regarding Fig. 5 and the need to use percentiles rather than absolute values. Although the central Arctic experienced

unusually high precipitation relative to its climatology, the actual amounts remain low compared to lower-latitude regions.
As shown in Fig. 12c, some moisture loss does occur north of 80°N between Greenland and Svalbard. However, although this moisture loss is unusual for this region, its magnitude is relatively small (up to ~10 g kg^{-1}) compared to the substantially larger moisture losses occurring further south along the two transport pathways. Consequently, the central Arctic appears to exhibit comparatively weak moisture loss in the spatial distribution. We have added a sentence to discuss this:
'In the Arctic, moisture loss is observed west of Svalbard, and although highly unusual for the region, it remains relatively small in magnitude compared to the larger losses occurring at lower latitudes.' See lines 397-399 on page 20.

Q: Lines 364-365: If that is the case, why not track the parcels backward in time for more than 7 days?
A: We thank the referee for this comment, which helped us improve the discussion of moisture uptake within the Eurasian AR. We have modified the sentence to read: *'The Eurasian AR derived its moisture from continental Eurasia (Fig. 12). While moisture uptake was most pronounced over central and eastern Europe, a secondary uptake region is evident east of the Ural Mountains over western Siberia. The close spatial alignment between moisture uptake and loss regions suggests that a substantial fraction of moisture is locally recycled within the AR (Nusbaumer and Noone, 2018), indicating that parcels already carried elevated moisture content when being incorporated into the AR airmass and highlighting the role of long-range transport in sustaining AR moisture content.'* See lines 454-458 on page 24.
LAGRANTO back trajectories are computed for 9 days. The trajectory length used in the manuscript is then selected based on the AR lifecycle (Atlantic or Eurasian) and the parcel property evolution (Fig. 11 for different trajectory lengths; not shown in the manuscript), as described in the Methods section lines 183-187 on pages 6-7. Extending the trajectories further did not provide additional insight, as the key features of the parcel evolution remain unchanged.

Q: Line 366: Should be decreasing pressure.
A: We thank the referee for pointing this out. The text has been corrected.

Q: Lines 398–400: This is consistent with the Arctic AR trajectory-clustering results shown in Fig. 7d of Ma et al. (2025). They show that ARs that travel along the U.S. East Coast or the western Atlantic before entering the Arctic through the Atlantic pathway tend to be associated with enhanced moisture uptake from the warm waters of the Gulf Stream
A: We thank the referee for this suggestion. We have modified the relevant section as follows: '*These parcels originate south of 40°N and travel northward along the eastern*

coast of the USA, drawing moisture predominantly from the warm waters of the Gulf Stream (Fig. 9). This aligns with previous studies showing that Arctic ARs of subtropical origin propagating through the Atlantic sector acquire moisture from the western North Atlantic (Ma et al., 2025).' See lines 441-444 on page 23.